

Interaction of Ultraintense Laser Pulses with an Underdense, Preformed Plasma Channel

V. Malka, J. Faure, J. R. Marquès, F. Amiranoff, C. Courtois, Z. Najmudin, K. Krushenick, M. R. Salvati, and A. E. Dangor

Abstract—We report on experimental results regarding the propagation of ultraintense laser pulses in a preformed plasma channel. In this experiment, the long (4-mm) fully ionized plasma channel created by the amplified spontaneous emission (ASE) was measured by interferometry before and after the propagation of the short laser pulse. Forward spectra show a cascade of Raman satellites, which merge with one another when the laser power was increased up to critical power for relativistic self-focusing P_c . The number of filaments measured by interferometry increases when the laser power increases. High conversion efficiency ($\approx 10\%$) of second harmonic generation was observed in the interaction.

Index Terms—Laser particule acceleration and plasma guiding, laser plasma interaction, relativistic self-focusing.

I. INTRODUCTION

THE propagation over a long distance of high-intensity laser beams in a plasma is crucial for laser plasma acceleration schemes [1]–[3], X-ray laser [4], high harmonics generation [5], and in inertial confinement fusion (ICF) with the fast ignitor scheme [6]. All of these schemes depend on the interaction length, which is typically limited by laser diffraction, to a few times the Rayleigh length. Various mechanisms can help to overcome this limitation. Relativistic and ponderomotive self-channeling are the natural way to do this, but they are not easy to obtain. Self-guiding in a preformed channel seems to be the most promising method to achieve propagation lengths of the order of several times the Rayleigh length. Recent experiments have proven the feasibility of this idea [7]–[11]. Intense electromagnetic waves propagating in an underdense uniform plasma can also excite intense relativistic plasma waves via the self-resonant wakefield instability (SRWI) [12]–[14] suitable for particle acceleration [15]–[19]. The maximum energy that an electron can get from the relativistic plasma waves (RPW) is proportional to the product of the RPW amplitude and the dephasing length (the length over which electrons stay in an accelerating arch of the relativistic plasma waves). In order to

Manuscript received September 30, 1999; revised January 31, 2000. This work was supported by the EPSRC, the Human Capital and Mobility Program, and the European TMR, under Contract ERBFMGECT950044.

V. Malka, J. Faure, J. R. Marquès, and F. Amiranoff are with LULI, UMR 7605, CNRS-CEA, Ecole Polytechnique-Université Pierre et Marie Curie, 91128 Palaiseau Cedex, France.

C. Courtois is with LPGP, UMR 8578, CNRS, Université Paris XI, 91405 Orsay, France.

Z. Najmudin, K. Krushenick, M. R. Salvati, and A. E. Dangor are with Imperial College, SW7 2BZ, London, U.K.

Publisher Item Identifier S 0093-3813(00)08795-6.

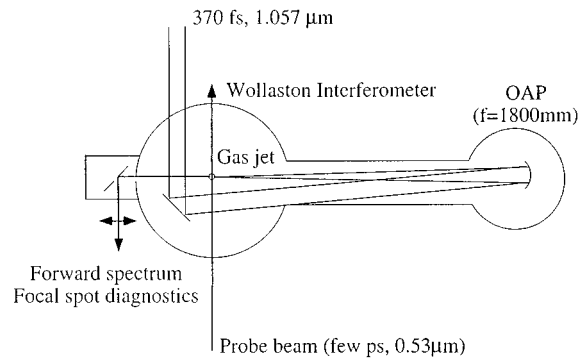


Fig. 1. Experimental setup.

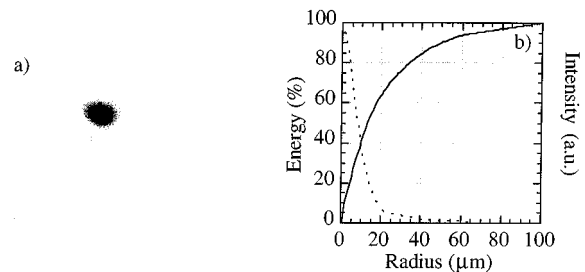


Fig. 2. (a) Focal spot image. (b) Fraction of energy contained inside a circle of radius r .

obtain the maximum energy from the waves, the electron must travel in a long and intense RPW. To achieve this with laser schemes, the laser pulse needs to be guided at high intensity. The interaction of an intense laser pulse with an underdense plasma is also of interest in the “fast ignitor” fusion concept. In this scheme, it is required to deliver a short, intense laser pulse to the (imploded) dense laser-fusion capsule. The intense pulse must propagate through a very long (a few millimeters) region of underdense plasma, and this propagation may be hampered by forward Raman scattering (FRS). Review papers on plasma guiding and plasma based accelerators can be found in [3] and [20].

In this paper, we present some recent experimental results on the propagation and the interaction of a short and intense laser pulse in a well-defined preformed plasma channel. Propagation was studied from interferograms, whereas interaction was studied from the FRS spectra. We also show that the second harmonic light is generated in the plasma channel and scattered

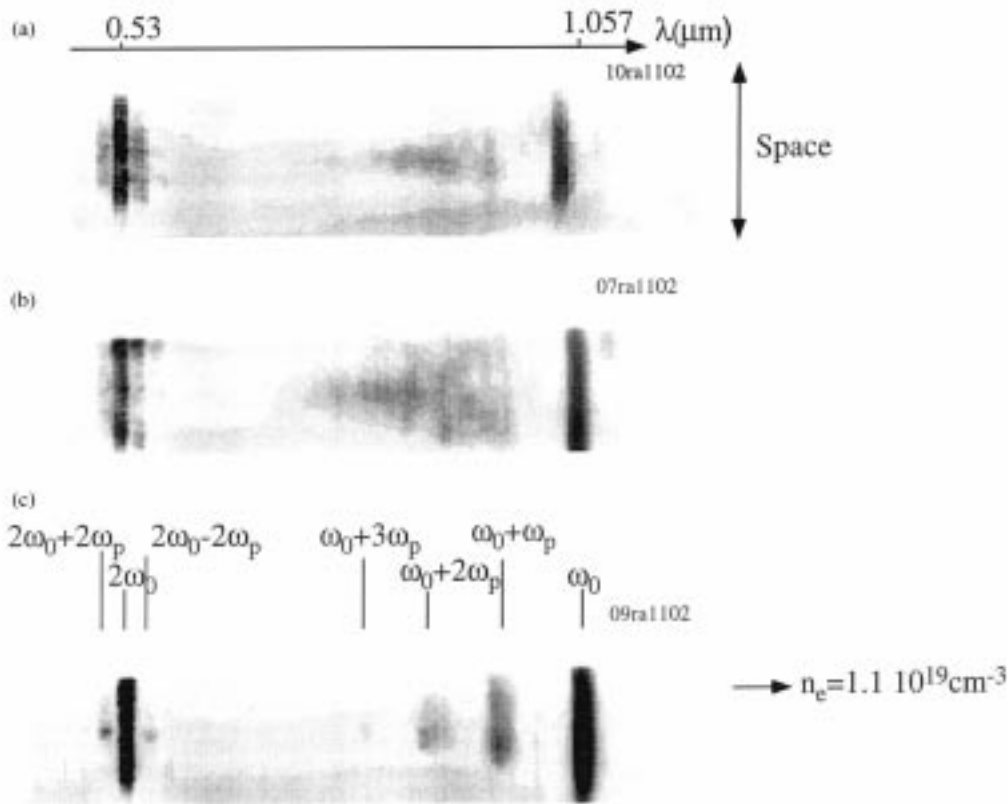


Fig. 3. Images of forward transmitted spectra obtained with a backing pressure of 60 bars, for a given energy of 10 J and for 370 fs (a), 3 ps (b), and 7 ps (c).

off the RPW, as evidenced by the observation of Stokes and anti-Stokes satellites in the forward Raman spectra.

II. EXPERIMENTAL RESULTS

The experiment described here was performed at LULI with the TW laser operating at $1.057 \mu\text{m}$ in the chirped-pulse amplification (CPA) mode. In this configuration, the laser provided up to 10 J (on target) in 370-fs pulses. The laser beam was focused onto the edge of a gas jet with a $f/22$ off-axis parabola after propagation in vacuum. The experimental setup is presented in Fig. 1. The focal spot was imaged with $12\times$ magnification on to an 8-bit charge-coupled device (CCD) camera with $5\text{-}\mu\text{m}$ spatial resolution. The laser distribution at full energy (10 J) at the focal plane is a Gaussian function with a waist (FWHM) of $20 \mu\text{m}$. In Fig. 2, we present the focal spot image [Fig. 2(a)] and the fraction of energy contained inside a circle with of radius r [Fig. 2(b)]. This corresponds to typical powers of 20 TW and to on-target intensities I_o of the order of $2\times 10^{18} \text{ W/cm}^2$. The measured Rayleigh length was 2 mm. To avoid refraction induced by ionization processes [21], [22], the laser beam was focused onto the sharp edge of a 4-mm diameter laminar plume of helium gas from a pulsed, supersonic gas jet located 2 mm below the focal region. The nanosecond prepulse, generated by using amplified spontaneous emission (ASE), with an estimated intensity of few 10^{14} W/cm^2 is intense enough to fully collisionally ionize helium and to create a channel over the whole length of the helium gas jet (4 mm). The electron density in the gas jet was controlled by changing the backing pressure of the jet. The neutral density

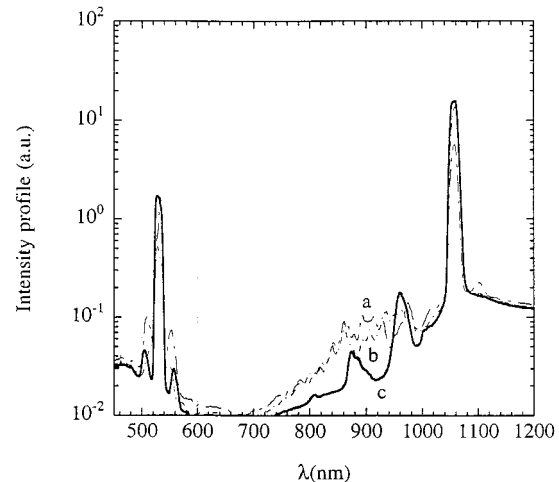


Fig. 4. On-axis corrected intensity profiles of spectra presented in Fig. 3.

profile was characterized before the experiment [23]. The interaction density was measured through the frequency shift ($n\omega_p$) of the anti-Stokes sidebands created by FRS, whereas the electron density profile is deduced from interferograms obtained from a green ($0.53\text{-}\mu\text{m}$) probe beam propagating at 90° to the laser axis, with a few picoseconds pulse duration.

The spectrum of the light transmitted in the forward direction was measured in the full $f/5$ cone angle and imaged at the entrance of an imaging spectrometer (100 lines/mm). This light was reflected by a silicate plate with a surface flatness of $\lambda/10$. The spectrum was detected with a 16-bit silicon CCD camera. A

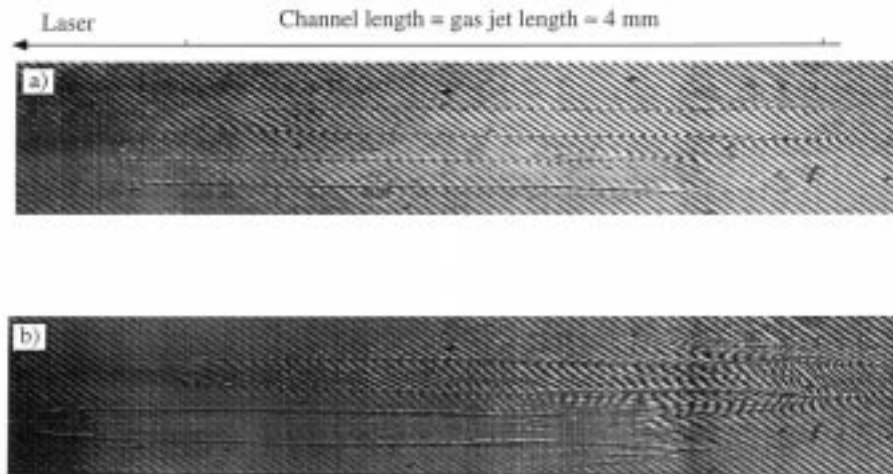


Fig. 5. Interferograms recorded 2 ps before [Fig. 4(a)] and 13 ps after [Fig. 4(b)] the main beam. The parameters are the same as those of Fig. 2(a).

bright blackbody source placed at the focal position of the pump laser was used to measure the overall transmission function of the optics and the spectral response of the CCD camera. This was used to correct the measured spectrum. Fig. 3 shows typical recorded forward spectra obtained with a backing pressure of 60 bars, for a given energy of 10 J and for 370 fs [Fig. 3(a)], 3 ps [Fig. 3(b)], and 7 ps [Fig. 3(c)]. The on-axis electron density deduced from frequency shift $n\omega_p$ of the anti-Stokes sidebands of the pump laser is $1.1 \times 10^{19} \text{ cm}^{-3}$ and corresponds to a critical power for relativistic self-focusing (as defined for a uniform plasma) of $P_c = 1.7 \text{ TW}$. The Stokes satellites are not visible on these spectra because of the poor efficiency of the silicon CCD above $1.1 \mu\text{m}$. The ratio between the laser power P_L and the critical power are then 17 [Fig. 3(a)], 2 [Fig. 3(b)], and 0.8 [Fig. 3(c)]. In the second harmonic, both Stokes and anti-Stokes satellites are visible. The electron density deduced from the position of the peaks of the satellites at $2\omega_0 \pm \omega_p$ is in agreement with those deduced at $\omega_0 + n\omega_p$. We observe that when P_L/P_c was increased, the satellites become broader and then merge with one another. In Fig. 4, we present the on-axis intensity profiles of these spectra after the overall spectral response was taken into account.

To obtain interferograms, the probe beam was sent into a Wolston interferometer and recorded with a 8-bit CCD camera. Interferograms presented in this paper correspond to time-integrated images of the plasma, recorded 2 ps before [Fig. 5(a)] and 13 ps after [Fig. 5(b)] the interaction beam. The plasma expansion is sufficiently slow to obtain, in most cases, well-defined fringes in spite of the duration of the probe pulse. The interferogram in Fig. 5 is obtained with the same parameters as those of Fig. 3(a). Each picture contains two identical images. In the first case, when the probe beam arrives before the TW laser pulse, we obtain an interferogram of the plasma created by the ASE. In this picture, the laser propagates from the right to the left. In the picture, we see the sharp shift in the fringes, which indicates a plasma-vacuum boundary. The radial plasma size is about $300 \mu\text{m}$ in diameter, and the plasma covers the whole length (4 mm) of the gas jet. The plasma length is limited by the dimension of the gas jet. The plasma expands radi-

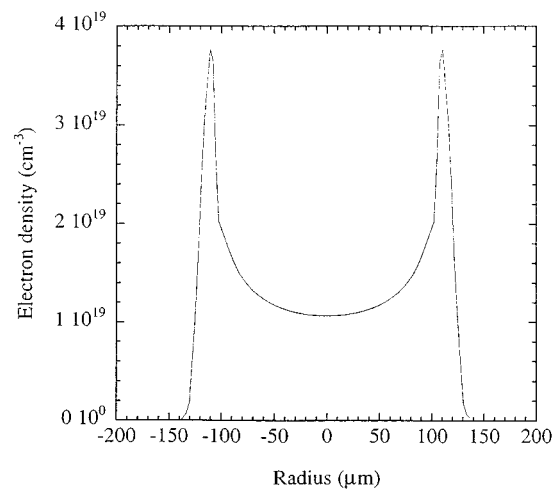


Fig. 6. Radial electron density deduced from the interferogram of Fig. 5(a).

ally over a distance of about $100\text{-}\mu\text{m}$ radius and is homogenous over the whole gas jet length. Fringes are clearly visible, and it is reasonable to suppose that the plasma is axisymmetric. We can then use Abel inversion to retrieve the radial density profile as presented in Fig. 6. The electron density increases from $1 \times 10^{19} \text{ cm}^{-3}$ on axis to $4 \times 10^{19} \text{ cm}^{-3}$ at a radius of $100 \mu\text{m}$. The on-axis electron density deduced from this interferogram is in good agreement with those deduced from the forward spectra. In the second case [Fig. 5(b)], we also observe [11], [24] at the beginning of the interaction zone, short filaments outside of the laser propagation axis that propagate over a distance of $\approx 1 \text{ mm}$. A main filament stays on the laser propagation axis over 3 mm. In this case, we cannot deduce the electron density profile using Abel inversion because the axisymmetric assumption is not justified. In the lower power case, only one long filament was observed.

In Fig. 7, we present an image obtained at $2\omega_0$, at 90° , to the laser propagation axis in that we see a long green filament that propagates over 3 mm. We point out here the fact that the TW laser beam is perfectly aligned along the channel center, because



Fig. 7. Second harmonic side images [same parameters as Fig. 2(a)].

the creation beam (ASE beam) is perfectly aligned with the TW laser beam.

III. DISCUSSION

In the experiments described in this paper, the RPW is excited by an intense pulse via the self-modulated wakefield SMW instability. In this regime, the strong electromagnetic pump wave (ω_o, k_o) decays into a plasma wave (ω_p, k_p) and two forward-propagating electromagnetic cascades at the Stokes $(\omega_o - n\omega_p)$ and anti-Stokes $(\omega_o + n\omega_p)$ frequencies [12]–[14], [25], [26]. Here, $\omega_p = (4\pi n_e c^2/m)^{1/2}$ is the plasma frequency and n is a positive integer. The signature of such a process is then visible in the presence of Stokes and anti-Stokes satellites in the spectrum of the transmitted light. We can estimate of the RPW amplitude, if we assume that the ratio of the harmonic Raman satellites is proportional to the harmonic content of the scattering plasma wave. The harmonic amplitude of the scattering μ_m as a function of the plasma wave amplitude $\delta n/n_o$, is given by [27]

$$(\mu_m/\mu_o) = (m^m/2^{m-1} \cdot m!) \cdot (\delta n/n_o)^m$$

where m is the number of the harmonic. Hence, the ratio between second and first harmonics is simply equal to the plasma wave amplitude. Values up to 6% were measured in the low laser power case. In the other cases, the satellites are so broad that is difficult to estimate this ratio.

In the high-power case, the main difference in the forward spectra near the propagation axis (where the electron density is constant) appears in the broadening of the Raman satellites. This is not surprising if we consider that the temporal envelope of the plasma wave is an increasing exponential function (at least at the beginning of the instability) $\exp(\Gamma t)$, where γ is the growth rate of the instability. The spectrum of such a wave has a width that is proportional to Γ . Furthermore, Γ scales as $I^{1/2}$ in the weakly relativistic limit. Hence, for the low-power case, the laser intensity is low and $\Gamma/\omega_p \ll 1$. This gives a narrow spectral peak at ω_p on the spectrum. This is as we observe on Fig. 3(c): in the high-power case, the intensity is larger, so is γ/ω_p , making the spectral peak wider. Physically, we can understand that when the growth rate becomes comparable to ω_p , the plasma wave can oscillate at nonresonant frequencies. Out of the propagation axis, the broad satellite [see the bottom of the Fig. 3(a)] could also be the signature of the propagation of light filaments in the high electron density region of the channel, as observed in the interferograms. These side beamlets can be produced in the self-focusing regime [28] or by Raman side scattering [29]. In the low laser power case ($P_L/P_C < 1$), the laser beam is self-guided by the plasma channel that satisfied the guiding condition.

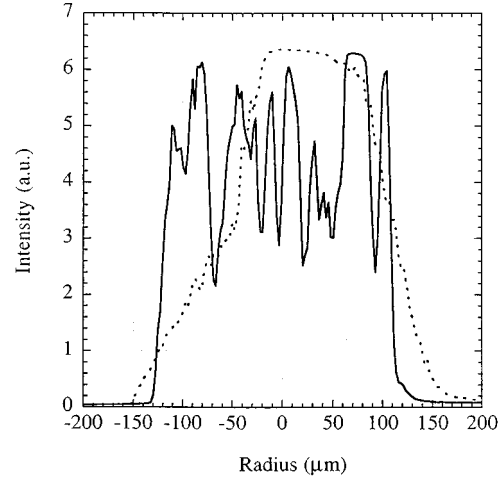


Fig. 8. Radial intensity profiles obtained from the forward Raman spectra at $2\omega_o$ and at ω_o [same parameters as Fig. 2(c)].

In previous experiments [30] ($I_o \approx 5 \times 10^{18}$ W/cm² and $f/3$ focusing), second harmonic light was observed in the forward direction with a conversion efficiency of 10^{-3} . The laser pulse was focused into the helium gas jet, whereas in the present case, the short pulse laser interacts directly with the preformed plasma. The measured second harmonic conversion efficiency in the cone angle of the laser is defined as the ratio between the integral signal at $2\omega_o$ and ω_o is of the order of 10%. The main mechanism to generate second harmonic is the presence of density gradients in the plasma. Physically, this is because of the laser-induced quiver motion of the electrons across a density gradient, which gives rise to a perturbation δn in the electron density at the laser frequency ω_o (as can be seen from the continuity equation). This density perturbation, coupled with the quiver motion of the electrons v_{osc} produces a source current J at the second harmonic frequency: $J = \delta n^* v_{osc} \propto \cos^2(\omega_o t) \propto \cos(2\omega_o t)$. For the transverse electron density gradient, the currents are phased to radiate predominantly in the forward direction. In this experiment, the source of the density gradient is mainly caused by relativistic or ponderomotive [31] self-focusing rather than laser ionization processes. This is shown by the observation (see Fig. 6) of the long filaments at $2\omega_o$ inside the plasma channel. Another confirmation of the production of second harmonic from density gradients appears clearly in the radial distribution measured in the forward spectra at $2\omega_o$. This distribution contains many hot spots, whereas the fundamental is homogeneous, as presented in Fig. 8. As mentioned in previous experiments [30], [32], the laser light is frequency-doubled passing the interaction region and scattered by the plasma wave, giving Stokes and anti-Stokes satellites at $2\omega_o \pm \omega_p$.

IV. CONCLUSION

In conclusion, we have presented experimental observations of the propagation of an ultraintense laser pulse in a preformed plasma channel. Propagation was investigated by using interferometry. In the high laser power case, many filaments produced at the beginning of the interaction zone were observed because of Raman side scattering or to beam breakup. Forward spectra shows a cascade of Raman satellites, which merge with one another, in the high laser power case. We also report on the observation of the forward scattering of second harmonic ($2\omega_0$) light from relativistic electron plasma waves driven by FRS. The generation of the second harmonic light is consistent with the presence of radial electron density gradients resulting from the radial ponderomotive force.

ACKNOWLEDGMENT

The authors wish to thank the LULI technical staff for their excellent support during the experiment, and A. Solodov and P. Mora for very useful discussions.

REFERENCES

- [1] T. Tajima and J. Dawson, "Laser electron accelerator," *Phys. Rev. Lett.*, vol. 43, pp. 267–270, 1979.
- [2] A. Modena, A. E. Dangor, Z. Najmudin, C. E. Clayton, K. Marsh, C. Joshi, V. Malka, C. B. Darrow, C. Danson, D. Neely, and F. N. Walsh, "Electron acceleration from the breaking of relativistic plasma waves," *Nature*, vol. 377, pp. 606–608, 1995.
- [3] E. Esarey, P. Sprangle, J. Krall, and A. Ting, "Overview of plasma-based accelerator concept," *IEEE Trans. Plasma Sci.*, vol. 24, pp. 252–288, 1996.
- [4] P. B. Corkum, N. H. Burnett, and F. Brunel, "Above-threshold ionization in the long-wavelength limit," *Phys. Rev. Lett.*, vol. 62, pp. 1259–1263, 1989.
- [5] X. F. Li, A. L'Huillier, M. Ferray, L. A. Lompre, and G. Mainfray, "Multiple Harmonic generation in rare gases at high laser intensity," *Phys. Rev. A*, vol. 39, pp. 5751–5760, 1989.
- [6] M. Tabak, J. Hammer, M. E. Glinsky, W. L. Kruer, S. C. Wilks, J. Woodworth, E. M. Campbell, M. D. Perry, and R. J. Mason, "Ignition and high gain with ultrapowerful lasers," *Phys. Plasmas*, vol. 1, pp. 1626–1634, 1994.
- [7] C. G. Durfee III and H. M. Milchberg, "Light pipe for high intensity laser pulses," *Phys. Rev. Lett.*, vol. 71, pp. 2409–2412, 1993.
- [8] C. G. Durfee III, J. Lynch, and H. M. Milchberg, "Development of a plasma waveguide for high-intensity laser pulses," *Phys. Rev. E*, vol. 51, pp. 2368–2389, 1995.
- [9] Y. Ehrlich, C. Cohen, A. Zigler, J. Krall, P. Sprangle, and E. Esarey, "Guiding of intensity laser pulses in straight and curved plasma channel experiments," *Phys. Rev. Lett.*, vol. 77, pp. 4186–4189, 1996.
- [10] K. Krushelnick, A. Ting, C. I. Moore, H. R. Burris, E. Esarey, P. Sprangle, and M. Baine, "Plasma channel formation and guiding during high intensity short pulse laser plasma experiments," *Phys. Rev. Lett.*, vol. 78, pp. 4047–4050, 1997.
- [11] C. E. Clayton, D. Gordon, K. A. Marsh, C. Joshi, V. Malka, Z. Najmudin, A. Modena, A. E. Dangor, D. Neely, and C. Danson, "Observation of self-channeling of relativistically-intense laser light in a very underdense plasma," *Phys. Rev. Lett.*, vol. 1, pp. 100–103, 1998.
- [12] N. E. Andreev, L. M. Gorbunov, V. I. Kirsanov, A. A. Pogosova, and R. R. Ramazashvili, "Self-resonant wake-field generation by intense laser pulse in plasmas," *JETP Lett.*, vol. 55, pp. 571–574, 1992.
- [13] T. M. Antonsen and P. Mora, "Self-focusing and raman-scattering of laser-pulses in tenuous plasmas," *Phys. Rev. Lett.*, vol. 69, pp. 2204–2207, 1992.
- [14] P. Sprangle, E. Esarey, J. Krall, and G. Joyce, "Propagation and guiding of intense laser-pulses in plasmas," *Phys. Rev. Lett.*, vol. 69, pp. 2200–2203, 1992.
- [15] A. Modena, A. E. Dangor, Z. Najmudin, C. E. Clayton, K. Marsh, C. Joshi, V. Malka, C. B. Darrow, and C. Danson, "Observation of Raman forward scattering in the relativistic regime," *IEEE Trans. Plasma Sci.*, vol. 24, pp. 289–295, 1996.
- [16] C. A. Coverdale, C. B. Darrow, W. L. Kruer, and S. V. Bulanov, "Modulations in Raman backscatter spectra due to interaction of short-pulse high-intensity laser with underdense plasma," *Phys. Rev. Lett.*, vol. 74, pp. 4659–4663, 1995.
- [17] D. Gordon, K. C. Tzeng, C. E. Clayton, A. E. Dangor, V. Malka, K. A. Marsh, A. Modena, W. B. Mori, P. Muggli, Z. Najmudin, and C. Joshi, "Observation of electron energies beyond the linear dephasing limit from laser-excited relativistic plasma wave," *Phys. Rev. Lett.*, vol. 80, pp. 10–13, 1998.
- [18] D. Umstadter, S. Y. Chen, A. Maksimchuk, G. Mourou, and R. Wagner, "Nonlinear optics in relativistic plasmas and laser wake field acceleration of electrons," *Science*, vol. 273, pp. 472–475, 1996.
- [19] C. I. Moore, A. Ting, K. Krushelnick, E. Esarey, R. F. Hubbard, B. Hafizi, H. R. Burris, C. Manka, and P. Sprangle, "Electron trapping in self-modulated laser wakefields by Raman backscatter," *Phys. Rev. Lett.*, vol. 79, pp. 3909–3912, 1997.
- [20] W. P. Leemans, C. W. Widders, E. Esarey, N. E. Andreev, G. Shvets, and W. B. Mori, "Plasma guiding and wakefield generation for second-generation experiments," *IEEE Trans. Plasma Sci.*, vol. 24, pp. 331–350, 1996.
- [21] V. Malka, E. D. Wispelaere, J. R. Marquès, R. Bonadio, F. Amiranoff, F. Blasco, C. Stenz, P. Mounaix, G. Grillon, and E. Nibbering, "Stimulated Raman backscattering instability in short pulse laser interaction with helium gas," *Phys. Plasmas*, vol. 3, pp. 1682–1688, 1996.
- [22] P. Monot, "Interaction laser-gaz en champ intense," Thèse de doctorat, de l'université Paris-sud, Centre d'Orsay, 1993.
- [23] V. Malka, F. Amiranoff, C. Coulaud, J. P. Geindre, V. Lopez, Z. Najmudin, and D. Neely, "Mesure des profils de densités d'atomes dans des jets de gaz à géométrie cylindrique," Rapport d'activité du LULI, vol. NTIS PB99-130 973, 1998.
- [24] Z. Najmudin, C. Clayton, A. E. Dangor, C. Danson, D. Gordon, C. Joshi, V. Malka, K. Marsh, A. Modena, P. Muggli, D. Neely, and F. N. Walsh, "Investigation of a channelling high intensity laser beam in underdense plasmas," *IEEE Trans. Plasma Sci.*, vol. 28, pp. 1056–1069, Aug. 2000.
- [25] D. W. Forslund, J. M. Kindel, and E. L. Lindman, "Theory of stimulated scattering processes in laser-irradiated plasmas," *Phys. Fluids*, vol. 18, pp. 1002–1023, 1975.
- [26] W. B. Mori, C. D. Decker, D. E. Hinkel, and T. Katsouleas, "Raman forward scattering of short-pulse high-intensity lasers," *Phys. Rev. Lett.*, vol. 72, pp. 1482–1485, 1994.
- [27] F. F. Chen, "Excitation of large amplitude plasma waves," *Phys. Scripta*, vol. T30, pp. 14–21, 1990.
- [28] F. Vidal and T. W. Johnston, "Electromagnetic beam breakup: Multiple filaments, single beam equilibria, and radiation," *Phys. Rev. Lett.*, vol. 77, pp. 1282–1285, 1996.
- [29] J. T. M. Antonsen and P. Mora, "Self-focusing and Raman scattering of laser pulses in tenuous plasmas," *Phys. Fluids B*, vol. 5, pp. 1440–1452, 1993.
- [30] V. Malka, A. Modena, Z. Najmudin, A. E. Dangor, C. E. Clayton, K. A. Marsh, C. Joshi, C. Danson, D. Neely, and F. N. Walsh, "Second harmonic generation and its interaction with relativistic plasma waves driven by forward Raman instability in underdense plasma," *Phys. Plasmas*, vol. 4, pp. 1127–1131, 1997.
- [31] C. E. Max, J. Arons, and A. B. Langdon, "Self-modulation and self-focusing of electromagnetic waves in plasmas," *Phys. Rev. Lett.*, vol. 33, pp. 209–212, 1974.
- [32] K. Krushelnick, A. Ting, H. R. Burris, A. Fisher, C. Manka, and E. Esarey, "Second harmonic generation of stimulated Raman scattered light in underdense plasmas," *Phys. Rev. Lett.*, vol. 73, pp. 3681–3684, 1995.

V. Malka, photograph and biography not available at the time of publication.

J. Faure, photograph and biography not available at the time of publication.

J. R. Marquès, photograph and biography not available at the time of publication.

F. Amiranoff, photograph and biography not available at the time of publication.

K. Krushenick, photograph and biography not available at the time of publication.

C. Courtois, photograph and biography not available at the time of publication.

M. R. Salvati, photograph and biography not available at the time of publication.

Z. Najmudin, photograph and biography not available at the time of publication.

A. E. Dangor, photograph and biography not available at the time of publication.